







Estimation of Low Rotation Frequency Based on Doppler Shift Observations

Yonghu Zhang¹, Lu Feng^{2*}, Jun Wu¹, Peng Wu²

¹Hunan Satellite Navigation Information Technology Co., Ltd., Changsha 410005, China

²School of Electronic Information and Electrical Engineering, Changsha University, Changsha 410022, China

Corresponding Author Email: fenglu@ccsu.edu.cn

<https://doi.org/10.18280/ts.400118>

ABSTRACT

Received: 21 October 2022

Accepted: 9 January 2023

Keywords:

GNSS, low speed rolling vehicle, doppler frequency shift, roll speed estimation

Rolling frequency measurement is an essential technology in attitude measurement of projectiles. For low rotation speed projectiles, the existing PLL methods have problems of complex loop parameter design and long algorithm convergence time, and usually need customization of GNSS receiver, resulting in an increase of application cost. In this paper, a method to estimate the roll frequency of projectiles by analyzing Doppler shift of Global Navigation Satellite System (GNSS) signals is proposed. The Doppler frequency shift observations are acquired in the state of single antenna installed on the side of cylindrical projectile. The roll frequency is extracted by analyzing signal frequency domain features. GNSS signals generated by the satellite signals simulation source are used to test the performance of this algorithm in low speed scenarios. Experiments on the rotary table are carried out to verify the method. Results of these experiments show that roll frequency estimation standard deviation of this method is less than 0.01Hz, when the Doppler shift measurement error is less than 3Hz. The method provides a new idea for the vehicle rotation attitude measurement, and effectively solves the problem of modifying the GNSS receiver with the signal energy for rolling frequency measurement, which greatly improves the application range of low-cost attitude measurement devices.

1. INTRODUCTION

The attitude information of projectiles is an important parameter in the navigation system. In order to ensure the stability of their flight, sounding rockets and intelligent ammunition projectiles usually maintain their own rotation during flight movement and their spinning movement directly affects the work of various attitude measurement devices [1, 2]. Common attitude information estimation methods are available including inertial navigation system (INS), geomagnetic sensor, GNSS receiver, etc. Inertial sensor has the advantages of low power consumption, good autonomy and easy integration, but the error of attitude measurement gradually accumulates with the extension of working time and cannot work continuously. At the same time, the inertial sensor also needs initial calibration, and its application cost is much higher than that of other posed methods. In addition, inertial sensor has a large volume, which requires more installation space. The high overload of projectile emission makes the inertial sensor often unable to work normally [3-5]. The geomagnetic field, like the earth's gravity field, is a benchmark existing in space, and its strength and direction constitute a function of the geographical location of the geomagnetic sensor, so it is also a common attitude measurement device. The error of measurement does not accumulate over time when geomagnetic sensors are used. It works unrelated to the movement of the projectile, and it has good performance on overload resistance. The low cost of use makes it widely used. However, it is susceptible to be influenced by external magnetic field and metal structure of the projectile. The anti-interference ability of geomagnetic sensors is poor, so it is usually used as an auxiliary means of attitude measurement

and combined with other sensors [6, 7].

Projectiles are usually equipped with GNSS receivers, which provides users with high precision spatio-temporal information under the condition of fast signal acquisition and stable signal tracking [8]. On the basis of these, highly cost-effective could be obtained by using GNSS receivers in high-precision attitude measurement. The problem of installation space limitation brought by the additional installation of inertial sensors or geomagnetic sensors could be solved to a great extent. As early as the 1990s, some scholars proposed the method of using GPS receivers to estimate flight attitude independently [8, 9]. The position and attitude information can be acquitted simultaneously by a GNSS receiver, so it can not only save the cost of using more other sensors, but also reduce the complexity of mechanical structure of projectiles.

Based on the GNSS receiver, the roll attitude can be measured by two modes: multi-antenna attitude measurement method and single-antenna attitude measurement method. In the multi-antenna mode, multiple antennas are usually installed at the same cross section of the rotating projectiles, so that at least one antenna receives satellite signals at any time. Some scholars proposed that the rolling attitude of the carrier can be judged by the amplitude correlation value of the satellite signals received by multiple antennas [10-12]. This method takes the carrier speed as the prior information to ensure the accurate realization of the subsequent attitude estimation algorithm. In this method, the signals received by multiple antennas are combined, but the signals between the antennas in the combined signal are easy to interfere with each other, and the signal noise of the combined signal increases compared with the single signal mode [13, 14].

In the single-antenna mode, the antenna is usually deployed on the side of the cylindrical projectile, and moving around the cross section together with the projectile. The spinning of projectile will bring a modulation effect to the GNSS signal received by the single antenna. Deng et al. [15] proposed to treat the rotating Doppler shift of sinusoidal law as the noise of fixed frequency and filter it through carrier loop filtering to keep the tracking of the relative movement of the receiver and the satellite, in the absence of roll frequency as prior information [16, 17]. The rotational attitude is estimated by analyzing the energy relationship between the received signal and the phase center of the antenna. Kim et al. [18] and Lee et al. [19] analyzed the carrier phase and carrier frequency bias induced by rotation and estimated the rotation frequency using the I and Q correlated summations of the correlators. Although the methods above can solve the problems of inter-antenna signal interference and reduce the mechanical structure complexity of the system, which are the key factors that affect performance of rotational attitude estimation by multi-antenna measurement, there are still some problems when the methods work at low roll frequency (such as sounding rocket, etc.). As the carrier phase is used to identify the rolling frequency, for the low roll frequency situation, the phase-locked loop parameter design is complex, and the signal detection accuracy is affected by the loop parameters. These problems will lead to loop unlocking and algorithm failure. The method of using GNSS signal energy to estimate the roll frequency needs to use the received GNSS signal amplitude information, but most of GNSS receivers cannot directly output amplitude of the signals. If the real-time signal amplitude should be output as a measurement, the receiver should be customized that would greatly increase the cost of the receiver. This makes the method is only suitable for application scenarios of high-cost customized receivers, and less applicability for non-customized applications. In addition, high-order phase-locked loop is used to track the changing of rolling frequency. In the case of low speed, a long tracking period is needed, which affects the real-time performance of the algorithm.

In view of the problems above, this paper takes single micro-strip antenna mounted on low rolling speed vehicle as the research object, and analyzes the periodic oscillation characteristics of real-time Doppler shift measured when the phase center of the receiver antenna moves in a circular motion on the side of the vehicle. The correlation between Doppler shift and vehicle roll frequency is discussed. The rolling frequency of the vehicle is estimated by Doppler frequency shift observations which can be output in real time by a general receiver.

The remainder of this paper is organized as follows. The second part presents the time-frequency domain analysis of the Doppler frequency shift. Then the composition and influencing factors of Doppler shift are discussed. The third part presents a roll frequency estimation method based on real-time Doppler shift observation. In the fourth part, the proposed rolling frequency estimation algorithm is verified in multiple dynamic scenarios, and performance of the rolling frequency estimation under different Doppler shift observation noise conditions are discussed. According to the analysis, it can be seen that the algorithm proposed in this paper can effectively identify the rolling frequency of the low rolling frequency vehicle. Differential operation and FFT processing of Doppler frequency shift are needed in the algorithm, which are less computationally intensive, to ensure the real-time performance of the algorithm.

2. ANALYSIS OF THE DOPPLER FREQUENCY SHIFT AMOUNT OF THE ROLLING VEHICLE

In order to estimate the rotation frequency of the vehicle by rotation Doppler frequency shift measurement, a single antenna of the GNSS receiver was mounted on the side of the vehicle. So the antenna phase center will rotate with the vehicle, and then the Doppler shift measurements will change in sine law. The changing rule could be used to judge the rotation frequency of the vehicle. Besides, the rotation plane of the antenna and LOS (line of sight vector) is at a certain angle, which has a certain influence on the amplitude of Doppler shift measurements. The geometric relationship between the receiver and the GNSS satellite is shown in Figure 1.

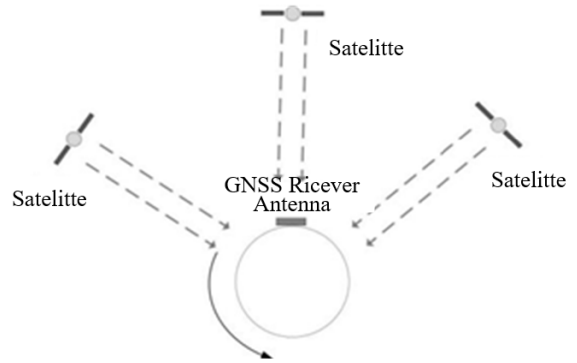


Figure 1. Schematic diagram of single antenna mounted on rolling vehicle

The relationship between ECEF (Earth-Centered Earth-Fixed) $OXYZ$ and topocentric coordinate system of the vehicle $O_1X_1Y_1Z_1$ is shown in Figure 2.

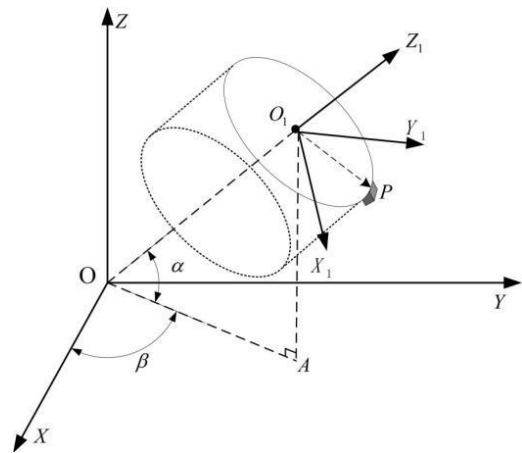


Figure 2. Geometric relationship between the ECEF coordinate system and the topocentric coordinate system of the vehicle

In topocentric coordinate system $O_1X_1Y_1Z_1$, the center of the vehicle is work as the coordinate origin which denoted by O_1 . The phase center of the non-omnidirectional antenna is located at the side point P of the rotating vehicle. Its rotation plane is the cross section of the vehicle. When the vehicle rotates, the phase center of the antenna will rotate on the circumference with O_1 as the center and r as the radius (that is the radius of the cylindrical carrier). The translational direction vector of the vehicle is consist with O_1Z_1 .

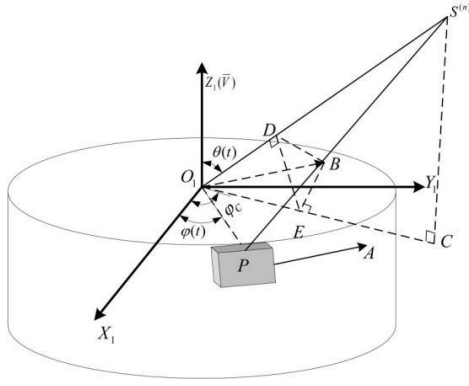


Figure 3. Analysis of Doppler frequency shift observed in topocentric coordinate system

The GNSS receiver obtains the accurate satellite position and speed on each observation epoch, and calculates the signal Doppler frequency shift by least squares. The calculation results include the satellite clock difference, the receiver clock difference, the ionosphere delay, the troposphere delay and so on. Figure 3 shows the diagram of Doppler frequency shift observation analysis when single antenna rotates with the vehicle in topocentric coordinate system. The real-time antenna phase center is denoted by P . And \overline{PA} is the circular motion velocity vector of the antenna phase center, $|\overline{PA}| = r \cdot 2\pi f_r$. With axis O_1X_1 as the rolling phase 0° , then the real-time rolling phase is $\varphi(t)$. $\overline{PS}^{(n)}$ is the distance between the phase center of the antenna and satellite n . $O_1S^{(n)}$ is the distance between the center of the rotation plane of and satellite n . Vector \overline{PA} is translated to $\overline{O_1B}$ in plane $X_1O_1Y_1$, and making \overline{BD} as a perpendicular from B to line of sight vector $\overline{O_1S}^{(n)}$, then $\overline{O_1D}$ is the projection of rotation velocity vector \overline{PA} on LOS. With the rotation of the vehicle, the rotational speed vector \overline{PA} changes, then $|\overline{O_1D}|$ changes with real-time roll angle $\varphi(t)$. When $\overline{O_1P}$ coincides with $\overline{O_1C}$ (the projection of LOS in plane $O_1X_1Y_1$), the minimum value of $|\overline{O_1D}|$ is obtained, and the vehicle roll angle is φ_c .

In order to get the expression of $|\overline{O_1D}|$, a perpendicular line from B to O_1C is made, the foot of perpendicular is E , then E and D are connected. Because $O_1Z_1 \perp X_1O_1Y_1$, then $O_1Z_1 \perp BE$. Besides $BE \perp O_1C$, so $BE \perp Z_1O_1C$, then $BE \perp O_1S$ can be deduced. BD is perpendicular to O_1S , thus vector O_1S is perpendicular to plane BDE , and that ED is perpendicular to O_1S could be obtained. Because \overline{PA} is the velocity direction of the circular movement of the antenna, that is, the tangent direction of the point P , so \overline{PA} is perpendicular to $\overline{O_1P}$, and $\overline{O_1B} \parallel \overline{PA}$, that makes $\angle BO_1P$ to be a right Angle in $\triangle BO_1E$.

When the antenna phase center rotating with the vehicle, $\varphi_c = 2\pi f_r t_c + \varphi_0$ donates as the real-time roll angle corresponding to $\overline{O_1C}$, where f_r is roll frequency of the vehicle and t_c is the time required for phase center of the antenna rotates coincide with the projection of the line of sight vector in $O_1X_1Y_1$. The angle between $\overline{O_1P}$ and $\overline{O_1C}$ can be deduced as

$$\Delta\varphi(t) = \varphi(t) - \varphi_c = 2\pi f_r t - 2\pi f_r t_c \quad (1)$$

where, $\angle BO_1E = 90^\circ - \Delta\varphi(t)$, therefore in the right triangle BEO_1 .

$$|O_1E| = |O_1B| \cdot \cos[90^\circ - \Delta\varphi(t)] \quad (2)$$

The real-time value of $|O_1D|$ can be obtained from the angle $\theta^{(n)}(t)$:

$$\begin{aligned} |O_1D| &= |O_1E| \cdot \sin[90^\circ - \theta^{(n)}(t)] \\ &= |O_1B| \cdot \cos[90^\circ - \Delta\varphi(t)] \cdot \cos[90^\circ - \theta^{(n)}(t)] \\ &= |O_1B| \cdot \sin[\Delta\varphi(t)] \cdot \sin[\theta^{(n)}(t)] \\ &= |PA| \cdot \sin[\Delta\varphi(t)] \cdot \sin[\theta^{(n)}(t)] \end{aligned} \quad (3)$$

The function of time $F_D(t)$ is used to represent the real-time Doppler shift of the GNSS signal, $F_{DL}(t)$ represents the Doppler shift caused by the relative movement of the vehicle and the satellite, that is, the changing projection of the relative motion speed on the LOS. $F_{DR}(t)$ represents the Doppler shift caused by the rotation of the vehicle, that is, the changing projection of the rotation speed vector on the LOS. Then we have:

$$F_D(t) = F_{DL}(t) - F_{DR}(t) \quad (4)$$

It can be seen from Eqns. (3) and (4) that the real-time Doppler frequency shift observation consists of two parts. One part is $F_{DR}(t)$, which changes sinusoidally with the circular motion of the antenna, and its oscillation frequency is consistent with the vehicle rotation frequency f_r . The instantaneous value of $F_{DR}(t)$ is affected by $\theta^{(n)}(t)$, which can be obtained from the rotation plane normal vector $\overline{O_1Z_1}$ and the LOS vector $\overline{O_1S}^{(n)}$ of the satellite n :

$$\theta^{(n)}(t) = \arccos \frac{\overline{O_1Z_1} \cdot \overline{O_1S}^{(n)}}{|\overline{O_1Z_1}| \cdot |\overline{O_1S}^{(n)}|} \quad (5)$$

When the vehicle moves, assume that the angle of attack is 0. Then its rotation plane normal vector is usually consistent with its velocity direction. From Eq. (5), $\theta^{(n)}(t)$ changes with the vehicle movement with time.

After the initial launch of the projectile, the analysis of its motion without power can be obtained.

$$F_{DL}(t) = \frac{f_c [v^{(s)}(t) - v_L(t)]}{c} = \frac{f_c}{c} \cdot [v(t_0) + a(t - t_0)] \quad (6)$$

where, f_c is the carrier frequency of GNSS, light speed is $c = 3 \times 10^8 (m/s)$. t_0 is the initial moment of free fall for the powerless spinning vehicle after launch; t is any moment before the vehicle stops moving after t_0 . $v(t_0)$ is the initial relative velocity. $\overline{a}(t)$ is the projection of the acceleration of the vehicle on the LOS vector under powerless state. In the unpowered state, the acceleration of the vehicle is affected by factors such as gravity acceleration and wind resistance, and the acceleration changes with time.

In this paper, the acceleration change caused by other factors except gravity acceleration is treated as part of the Doppler shift measurement noise, thus $\overline{a}(t)$ is considered as a constant vector. \mathbf{H} is set as the unit observation vector matrix. If the coordinate of the visible satellite n in topocentric

coordinate system is $s^{(n)}(x^{(n)}, y^{(n)}, z^{(n)})$, and the pseudo-distance observation amount is $\rho^{(n)}(t)$, then we have:

$$\mathbf{H} = \begin{bmatrix} \frac{\partial \rho^{(n)}}{\partial x} \\ \frac{\partial \rho^{(n)}}{\partial y} \\ \frac{\partial \rho^{(n)}}{\partial z} \end{bmatrix} = \frac{\mathbf{1}}{\rho^{(n)}(t)} \begin{bmatrix} x_0 - x^{(n)} \\ y_0 - y^{(n)} \\ z_0 - z^{(n)} \end{bmatrix} \quad (7)$$

Compared to the vehicle rotation vector $\overline{O_1 P}$ changing, the unit observation vector \mathbf{H} can be regarded as constant within a short observation epoch. According to Eq. (4), the Doppler frequency shift caused by the vehicle rotation is:

$$F_{DR}(t) = |PA| \cdot \sin[\Delta\varphi(t)] \cdot \sin[\theta^{(n)}(t)] \quad (8)$$

3. ESTIMATE THE ALGORITHM BASED ON THE ROLLING SPEED OF DOPPLER FREQUENCY SHIFT

After the GNSS signal received in the rolling state of the vehicle is processed by base-band processor, the real-time Doppler shift observation can be measured. According to Eq. (6), the $F_{DL}(t)$ part of Doppler frequency shift measurement is related to the relative motion speed and acceleration of the vehicle center of mass and the satellite, but not to the rotation of the vehicle. That is, in a certain time, the first order differential of $F_{DL}(t)$ is the acceleration of the relative motion of the two. The first order differential is constant when the acceleration is constant.

In combination with GNSS signal Doppler frequency shift, satellite position, receiver position, and Doppler frequency shift can be supposed continuously, the first derivative of Eq. (4) with respect to time is obtained:

$$\frac{dF_D(t)}{dt} = \frac{dF_{DL}(t)}{dt} - \frac{dF_{DR}(t)}{dt} \quad (9)$$

With the effect of gravity acceleration is the only considered factor when the vehicle flies without power, then $\overline{a}(t) = \overline{a}$ is a constant vector, thus:

$$\frac{dF_{DL}(t)}{dt} = \frac{d\left\{\frac{f_c}{c} \cdot [v(t_0) + \overline{a}(t-t_0)]\right\}}{dt} = \frac{f_c}{c} \cdot \overline{a} \quad (10)$$

$F_{DR}(t)$ in Doppler shift measurement of the GNSS signal is unrelated to the relative motion of the vehicle and the satellite. The first order differential of $F_{DR}(t)$ is the projection of the acceleration of the circular motion of the receiver on the LOS, whose variation is sinusoidal, and the fluctuation amplitude is proportional to $\theta^{(n)}(t)$. The first order differentiation of $F_{DR}(t)$ will show the vehicle roll frequency characteristic.

$$\frac{dF_{DR}(t)}{dx} = \frac{d\left\{|PA| \cdot \sin[\Delta\varphi(t)] \cdot \sin(\theta^{(n)})\right\}}{dt} = |PA| \cdot \sin(\theta^{(n)}) \cdot \cos[\Delta\varphi(t)] = |PA| \cdot \sin(\theta^{(n)}) \cdot \cos[2\pi f_r t - 2\pi f_r t_c] \quad (11)$$

During the process of differentiation in Eq. (11), $\theta^{(n)}(t)$ is also a time-varying function, but the changing rate is much smaller than the variation rate of Doppler shift caused by the rotation of the antenna, so it is considered as constant in this paper.

Eqns. (9)-(11) show that, in the first-order differential of Doppler frequency shift observations, the part formed by the relative motion of the vehicle and the satellite (Eq. (10)) is a constant; the part formed by the rotational motion of the spinning vehicle (Eq. (11)) contains the alternating component with frequency f_r . This component can be obtained by subtracting the average of first-order differential of Doppler frequency shift observations. Then, the rotation frequency f_r of the spinning vehicle can be derived from the alternating component in the frequency domain. After calculating the statistical average value of the first-order differential of the measured Doppler frequency shift, the constant part $\frac{f_c}{c} \cdot \overline{a}$ can be obtained.

Then subtracting this constant from the first-order differential of the Doppler shift observation, the projection of the velocity of the rotation vector on the line of sight vector (Eq. (11)). After frequency domain analysis, the vehicle roll frequency f_r could be obtained.

Eq. (8) shows that the amplitude of the sinusoidal fluctuation brought by the vehicle rotation changes with angle between the antenna rotation plane normal vector and the line of sight vector of the satellite n. The larger the angle of the two vectors, the greater the vibration amplitude will be. The maximum value of the amplitude is $r \cdot 2\pi f_r$.

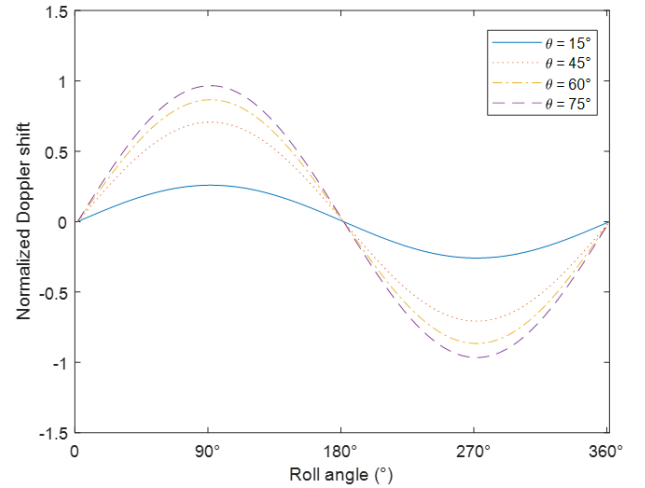


Figure 4. The relationship curve between Doppler frequency shift and $\theta^{(n)}(t)$

Figure 4 shows the correlation curve of the Doppler shift and the change angle $\theta^{(n)}(t)$. As we can be seen from Figure 4, the Doppler shift amplitude of the GNSS signal caused by rotation changes when the angle between the sight vector and the velocity vector differ.

$\theta^{(n)}(t)$ is affected by the direction of the vehicle speed, the relative position of the satellite and the receiver during the flight of vehicle. When estimating the vehicle rotation frequency, it is usually desirable to obtain a larger Doppler shift, then the larger rolling speed projection amplitude will be needed. In order to make a larger spectral amplification. Therefore, in the algorithm, the angle of the vehicle speed direction and the line of sight vector is calculated in real time,

and the threshold and satellite Doppler frequency shift measurements are set and selected to estimate the subsequent vehicle rotation frequency more accurately. At the same time, in order to reduce the interference of Doppler shift measurement noise and wind resistance, the spectrum of first-order differential of Doppler shift observations that corresponded to satellite n will be smoothed, if $\theta^{(n)}(t)$ is Over the threshold.

In this algorithm, the receiver processes the GNSS signal in base-band processor, obtains the real-time ephemeris, satellite pseudodistance, Doppler shift, and uses the least-squares method to solve the real-time velocity vector $\overline{v}(t)$ of the receiver. The position of the satellite n $s^{(n)}(x^{(n)}, y^{(n)}, z^{(n)})$ obtained by the ephemeris and the phase center of the receiver antenna are used to solve the line of sight vector $\overline{O_1S^{(n)}}$, and then calculate the angle $\theta^{(n)}(t)$ between the line of sight vector $\overline{O_1S^{(n)}}$ and the velocity vector $\overline{v}(t)$. The satellites that meet the requirements according to the threshold θ_{TH} will be selected. The more satellites that meet the requirements of the threshold, the higher the accuracy of the rolling frequency estimation. Thus, as the previous inference, if $\theta^{(n)}(t)$ goes larger, the first-order differential frequency spectrum of the Doppler shifted sinusoidal fluctuation will be larger, then estimation of the roll frequency will be more accurate.

In i epochs, we can obtain the mean value of the first-order differential of Doppler frequency shift observations corresponding to the satellite that meets the requirements, and denoting it as $\overline{Doppler}^{(n)}$. The choice of epoch number i is related to the rolling frequency and signal sampling rate of different vehicles. In general case, i should cover multiple cycles of vehicle roll, and the more the number of coverage cycles, the more accurate the estimate. However, only because of the real-time requirement of the rolling frequency estimation and the unit observation vector is considered constant in a short time, the value of i should be considered in a compromise. The mean of first-order Doppler shift fraction within i epoch is subtracted, that is described in Eq. (10), and the first-order differential $F_{DR}(t)$ remains as described in Eq. (11). The Doppler frequency shift observation spectrum can be obtained by fast Fourier transform of this signal.

The maximum of the spectrum will be find, and the vehicle rolling frequency could be obtained by outputting the corresponding frequency point f_r .

4. EXPERIMENTAL VALIDATION OF THE ALGORITHM

To verify the effectiveness and accuracy of the proposed roll frequency estimation method, we performed experimental studies. The experiments are based on a set of self-developed GNSS receiver. The chip rectangular micro-strip antenna of receiver was installed on a rotating stage, then the rotation state of the vehicle could be simulated. The rotating stage is controlled by a set of programmed motor, and the rotation speed can be adjusted from 0~25 (round)/s, as shown in Figure 5(a) and (b). The self-developed receiver is stuck inside the rolling cylinder, and the rectangular micro-strip antenna is installed on the side surface of the rolling cylinder. The data that is collected real-time is transmitted to the PC terminal for storage through the wireless data transmission interface for subsequent processing. The whole set of rolling cylinder and receiving device were placed in the microwave black box.

GNSS signal could be simulated by a satellite signal simulation source. The GNSS signal transmitting antenna was used to transmit the generated GNSS signal in the microwave black box.

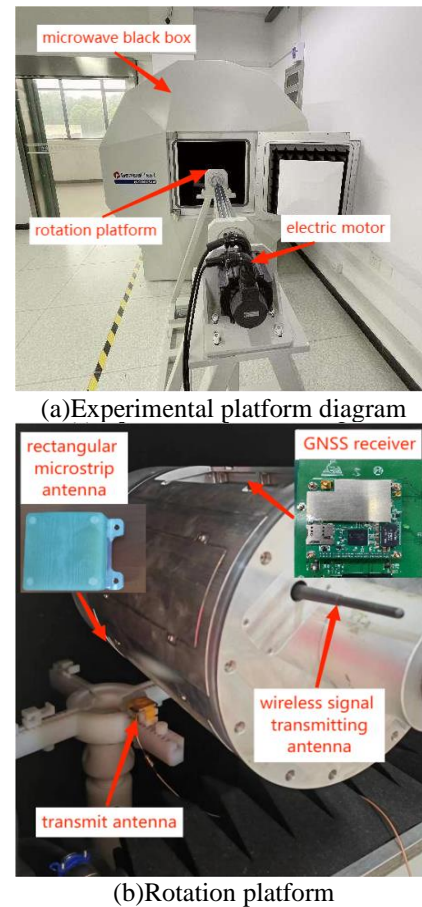


Figure 5. Rolling experimental apparatus

For testing the performance of algorithm proposed in this paper, there are five rotation states were selected, which are 0.1 r/s, 0.2 r/s, 0.5 r/s, 1 r/s, and 2 r/s. The sampling rate of Doppler frequency shift is 5 Hz, the number of observed epochs is no less than 200s, and the number of FFT operation points N is 2048.

Figure 6 shows the GNSS Doppler frequency shift observations as measured by the above experimental at roll frequency of 0.2 r/s. It can be seen from the figure that the Doppler frequency shift is sinusoidal due to the vehicle rotation, which is consistent with the previous analysis. Therefore, the rolling frequency information can be obtained by the frequency domain extraction method.

Figure 7 shows spectrum of the first-order differential of the Doppler shift observations obtained by the receiver from 3 satellites when the vehicle rolling rate is 0.2 r/s. As can be seen from the figure, the spectrum peak point appears in the spectrum at the rolling frequency of 0.2 Hz, and the frequency spectrum contains other frequency components. Because $\theta^{(n)}(t)$ is different in the three satellites, the peak amplitude of each spectrum in the figure is also different. It is clear that there is the largest $\theta^{(n)}(t)$ in spectrum of the first-order differential of the Doppler shift observations of satellite 3.

Based on the analysis of the experiments, it can be seen that the spectrum component related to the rotation frequency appears in the spectrum of the first order differential value of

Doppler shift observations, so the vehicle rotation frequency can be identified by this frequency spectrum. At the same time, the larger the angle of the line of sight vector and the velocity vector, the higher the accuracy of estimation of the roll frequency. The same experimental results can be obtained for all the satellites and other rolling rate that is no more than 3r/s.

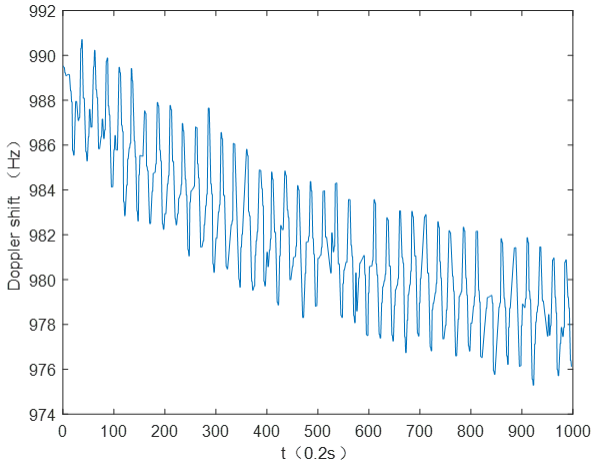
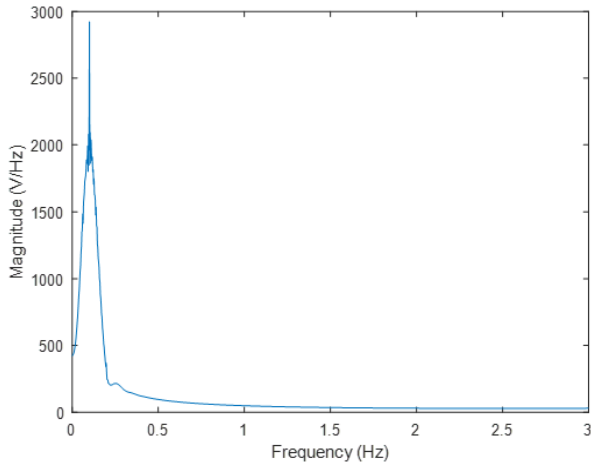
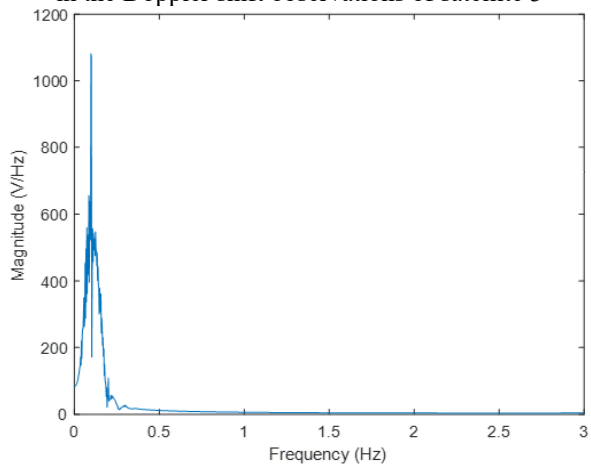


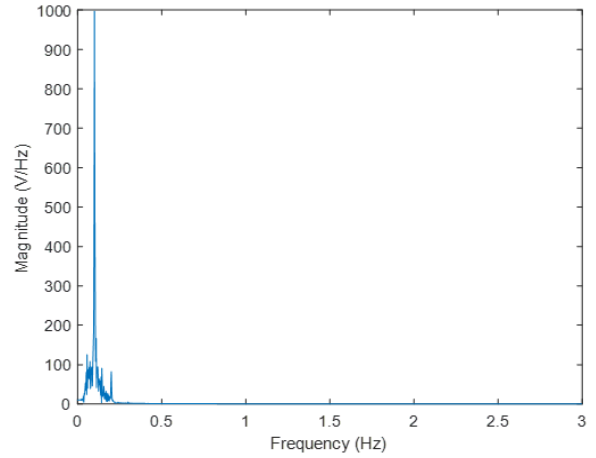
Figure 6. Rolling Doppler shift



(a) The first-order differential frequency spectrum of $F_{DR}(t)$ in the Doppler shift observations of satellite 3



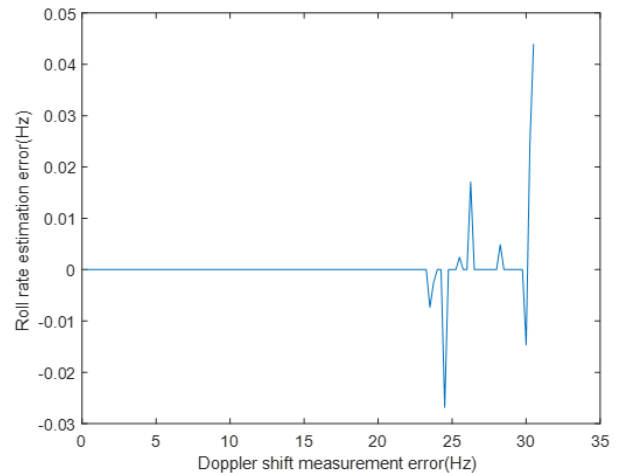
(b) The first-order differential frequency spectrum of $F_{DR}(t)$ in the Doppler shift observations of satellite 4



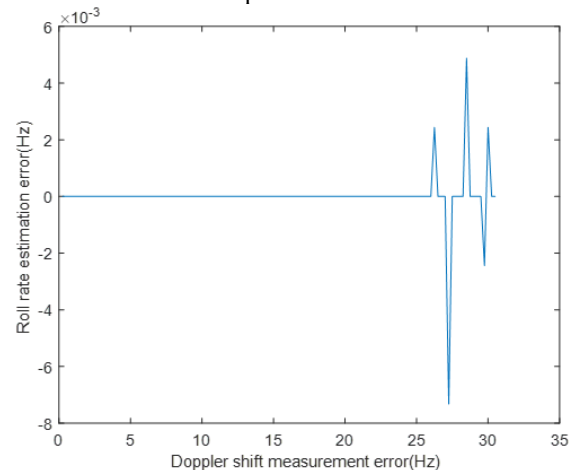
(c) The first-order differential frequency spectrum of $F_{DR}(t)$ in the Doppler shift observations of satellite 5

Figure 7. Spectrum of Doppler shift first-order differential

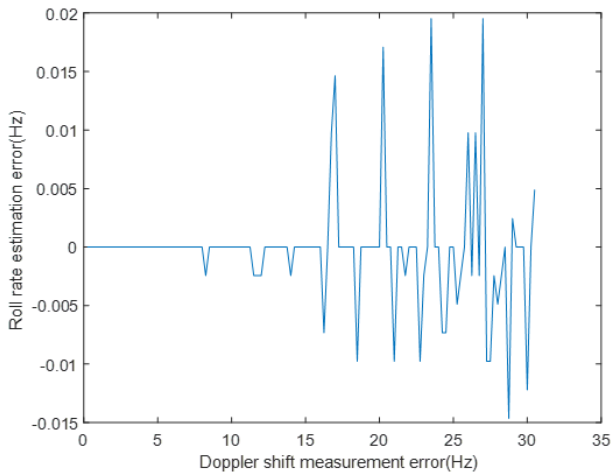
In the semi-physical experiment scenario set in this paper, we statistically analyze the performance of the algorithm, and the results are shown in Figure 8. Under the conditions of vehicle rotation speed of 0.1 r/s (0.1 Hz), 0.2 r/s (0.2 Hz), 0.5 r/s (0.5 Hz), 1 r/s (1 Hz) and 2 r/s (2 Hz), the proposed algorithm is used to estimate the rotation frequency, respectively. And the standard deviation of the Doppler shift measurement noise varies from 0 Hz to 30 Hz.



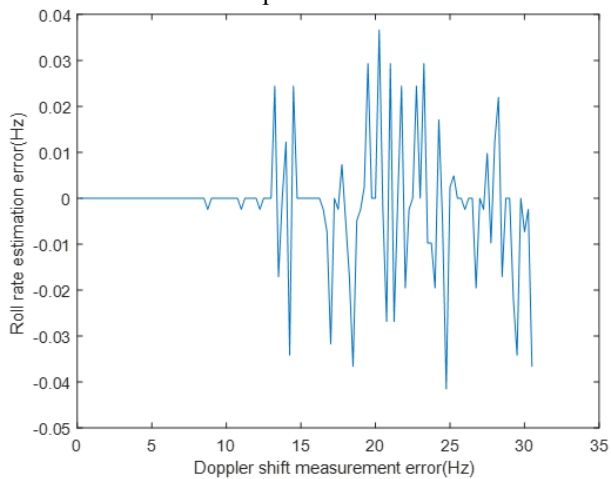
(a) Identification results of the roll frequency when the vector roll speed is 0.1 r/s



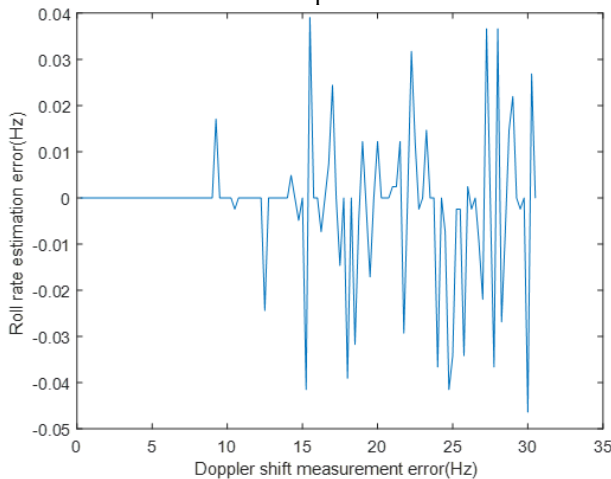
(b) Identification results of roll frequency when the vector roll speed is 0.2 r/s



(c) Identification results of roll frequency when the vector roll speed is 0.5 r/s



(d) Identification results of the roll frequency when the vehicle roll speed is 1 r/s



(e) Identification results of the roll frequency when the vehicle roll speed is 2 r/s

Figure 8. Results of estimation of vehicle rotation frequency under different measurement errors

It can be seen from the Figure 8 that the proposed algorithm can accurately estimate the vehicle roll frequency when the noise standard deviation of Doppler frequency shift measurement is less than 10 Hz. When the noise standard deviation is less than 10 Hz, the standard deviation of the estimated error is less than 0.01 Hz. In practical application, the current GNSS system, such as GPS, BDS, the Doppler frequency shift measurement error standard deviations are

probably less than 3 Hz. Besides, if some optimization method is adopted, the Doppler frequency shift measurement noise can be further reduced. Therefore, this algorithm is suitable for the low-speed vehicle roll frequency measurement in the existing GNSS system. When the vehicle rotation speed increases, the method of rotation speed estimation proposed in this paper is still effective, while the Doppler frequency shift sampling frequency is large enough (satisfying the sampling theorem).

5. CONCLUSION

This paper presents a method of estimating the vehicle rolling frequency. The single antenna was mounted on the side of the rotating vehicle, then the differential value of the Doppler shift changes in a sinusoidal rule could be obtained. Under the premise that the acceleration of the carrier can be regarded as constant, the fluctuation amplitude is associated with the angle between vector of the velocity and vector of LOS. Considering of this feature, the first-order differential of Doppler frequency shift observation is analyzed in frequency domain. The frequency point corresponding to the peak value of the spectrum is extracted and converted into the corresponding frequency output to obtain the vehicle rolling frequency. In this paper, semi-physical tests are carried out on vehicle with different rotational speeds. The test results show that the estimated error is less than 0.01 Hz, which is suitable for the current GNSS systems. Comparing with the multi-antenna estimation modes, the algorithm estimates the vehicle roll frequency based on the signals received by a single GNSS receiver antenna, and solves antenna signal interference problems and reduces the structural complexity. At the same time, the Doppler frequency shift observation used in this algorithm is the conventional output parameters of GNSS receivers. Compared with the customized development of the receiver, this algorithm can further reduce the cost of attitude measurement device without customized development, and ensures the simplicity and lightweight of the algorithm.

ACKNOWLEDGMENT

This paper was supported by Major projects of Changsha Science and Technology Bureau in 2020 (Grant No.: kq2011001), Key Research and Development Projects of Hunan Provincial Department of Science and Technology in 2022 (Grant No.: 2022GK2026), Hunan Natural Science Foundation Project (Grant No.: 2022JJ30636), Excellent Youth Program of the Scientific Research Program of the Department of Education of Hunan Province (Grant No.: 22B0838), Research Foundation of the Department of Natural Resources of Hunan Province (Grant No.: 2023-78), and Research Foundation of the Department of Natural Resources of Hunan Province (Grant No.: 2022-21).

REFERENCES

- [1] Silva, R.G.A.D., Damilano, J.G., Azevedo, J.L.F. (2013). A sensitivity investigation on the aeroelastic dynamic stability of slender spinning sounding rockets. *Journal of Aerospace Technology and Management*, 5: 15-26. <https://doi.org/10.5028/jatm.v5i1.192>
- [2] Yang, D., Gao, Y., Xiong, Y. (2008). Preliminary

- analysis of spinning solid rocket motor dynamics stability. *Journal of Propulsion Technology*, 29(1): 8-12.
- [3] Henkel, P., Günther, C. (2013). Attitude determination with low-cost GPS/INS. In *Proceedings of the 26th International Technical Meeting of the Satellite Division of The Institute of Navigation (ION GNSS+ 2013)*, Nashville, TN, USA, pp. 2015-2023.
- [4] Lacambre, J.B., Narozny, M., Louge, J.M. (2013). Limitations of the unscented Kalman filter for the attitude determination on an inertial navigation system. In *2013 IEEE Digital Signal Processing and Signal Processing Education Meeting (DSP/SPE)*, Napa, CA, USA, pp. 187-192. <https://doi.org/10.1109/DSP-SPE.2013.6642588>
- [5] Groves, P.D. (2015). Principles of GNSS, inertial, and multisensor integrated navigation systems [Book review]. *IEEE Aerospace and Electronic Systems Magazine*, 30(2): 26-27. <https://doi.org/10.1109/MAES.2014.14110>
- [6] Al-Rawashdeh, Y. M., Elshafei, M., & El-Ferik, S. (2016, July). Passive attitude estimation using gyroscopes and all-accelerometer IMU. In *2016 7th International Conference on Mechanical and Aerospace Engineering (ICMAE)*, London, UK, pp. 368-376. <https://doi.org/10.1109/ICMAE.2016.7549568>
- [7] Changey, S., Fleck, V., Beauvois, D. (2005). Projectile attitude and position determination using magnetometer sensor only. In *Intelligent Computing: Theory and Applications III*, Orlando, Florida, USA, pp. 49-58. <https://doi.org/10.1117/12.602099>
- [8] Van Graas, F., Braasch, M. (1991). GPS interferometric attitude and heading determination: Initial flight test results. *Navigation*, 38(4): 297-316. <https://doi.org/10.1002/j.2161-4296.1991.tb01864.x>
- [9] Wilson, G.J., Tonnemacher, J.D. (1992). A GPS attitude determination system. *The Journal of Navigation*, 45(2): 192-204. <https://doi.org/10.1017/S0373463300010699>
- [10] Doty, J.H. (2001). Advanced spinning-vehicle navigation-A new technique in navigation of munitions. In *Proceedings of the 57th Annual Meeting of The Institute of Navigation*, Albuquerque, NM, USA, pp. 745-754.
- [11] Doty, J.H., Anderson, D.A., Bybee, T.D. (2004). A demonstration of advanced spinning-vehicle navigation. In *Proceedings of the 2004 National Technical Meeting of the Institute of Navigation*, San Diego, CA, USA, pp. 573-584.
- [12] Doty, J.H., McGraw, G.A. (2003). Spinning-vehicle navigation using apparent modulation of navigational signals US6520448B1. US.
- [13] Wierzbicki, D., & Krasuski, K. (2015). Estimation of rotation angles based on GPS data from a UX5 Platform. *Measurement Automation Monitoring*, 61(11): 516-520.
- [14] Jang, J., Kee, C. (2009). Verification of a real-time attitude determination algorithm through development of 48-channel GPS attitude receiver hardware. *The Journal of Navigation*, 62(3): 397-410. <https://doi.org/10.1017/S0373463309005384>
- [15] Deng, Z., Shen, Q., Deng, Z. (2018). Roll angle measurement for a spinning vehicle based on GPS signals received by a single-patch antenna. *Sensors*, 18(10): 3479. <https://doi.org/10.3390/s18103479>
- [16] Zeng, G. (2015). Navigation and roll attitude determination technology by non-omnidirectional antenna under rotation condition. Doctoral thesis, Beijing Institute of Technology, China.
- [17] Liu, Y., Li, H., Du, X. (2019). Roll attitude measurement technique based on gps signal power. In *2019 IEEE International Conference on Unmanned Systems (ICUS)*, Beijing, China, pp. 280-284. <https://doi.org/10.1109/ICUS48101.2019.8995938>
- [18] Kim, J.W., Cho, J.C., Hwang, D.H., Lee, S.J. (2008). A roll rate estimation method using GNSS signals for spinning vehicles. *Journal of Institute of Control, Robotics and Systems*, 14(7): 689-694. <https://doi.org/10.5302/J.ICROS.2008.14.7.689>
- [19] Lee, S., Jin, M., Choi, H.H., Lee, S.J. (2016). Design of roll rate estimator using GPS signal for spinning vehicle. *Journal of Positioning, Navigation, and Timing*, 5(3): 109-118. <http://dx.doi.org/10.11003/JPNT.2016.5.3.109>